

## SÍNTESE, ESTUDO DE DOCAGEM E AVALIAÇÃO BIOLÓGICA DE DERIVADOS DA 4-AMINOANTIPIRINA-ISONIAZIDA COMO AGENTES HÍBRIDOS ANTIBACTERIANOS E ANALGÉSICOS

## SYNTHESIS, DOCKING STUDY, AND BIOLOGICAL EVALUATION OF 4-AMINOANTIPYRINE-ISONIAZID DERIVATIVES AS A HYBRID ANTIBACTERIAL AND ANALGESIC AGENTS

تحضير ودراسة الالتحام والتقييم البيولوجي لمشتقات 4-امينو انتيبيرين-ايزونزاييد كعوامل هجينة مضادة للبكتريا ومسكنة

MOHAMMAD, Abeer Essa<sup>1</sup>; MUHAMMAD-ALI, Munther Abduljaleel<sup>2\*</sup>; JASIM, Ekhlas Qanber<sup>3</sup>

<sup>1</sup> University of Basrah, College of Pharmacy, Department of Pharmaceutical Chemistry. Basra, Iraq.

<sup>2\*</sup> University of Basrah, College of Science, Department of Ecology. Basra, Iraq.

<sup>3</sup> University of Basrah, College of Science, Department of Pathological Analyses. Basra, Iraq.

\* Corresponding author

e-mail: munther.ali@uobasrah.edu.iq

Received 23 June 2022; received in revised form 26 August; 11 September 2022; accepted 02 October 2022

## RESUMO

**Introdução:** 4-aminoantipirina é um dos derivados pirazolona, expôs uma grande variedade de atividades biológicas como compostos antimicrobianos, analgésicos, antivirais, anti-inflamatórios e anticancerígenos. Um dos derivados importantes é a pirazolona híbrida que inclui dois compostos orgânicos ou inorgânicos ligados para produzir novos agentes farmacêuticos que podem possuir atividade igual ou diferente dos medicamentos originais. **Objetivo:** O objetivo desta pesquisa foi sintetizar novos compostos derivados de 4-aminoantipirina e testar sua atividade biológica. **Métodos:** A síntese de derivados de 4-aminoantipirina, que contêm estruturalmente dois metades heterocíclicas, pirazolona com anéis de oxadiazol, triazol ou tetrazol. As estruturas dos compostos foram identificadas por espectroscopia de <sup>1</sup>H-NMR e FT-IR. Os compostos desenvolvidos foram *in vitro* para testar sua atividade analgésica e atividade antibacteriana contra cepas bacterianas de gram (+) e gram (-). **Resultados:** Os testes de avaliação antibacteriana mostraram que alguns compostos deram boa atividade e outros não apresentaram atividade antibacteriana. A atividade analgésica indicou que os compostos sintetizados tinham potência promissora. A energia de ligação livre (S) dos compostos com a proteína 6B73 foi de -4,90 a -8,76 kcal/mol, enquanto a energia livre (S) com a proteína 5C1M foi de -4,94 a -9,21 kcal/mol. **Discussão:** Entre os compostos testados, verificou-se que os compostos 1a, 4b e 5a apresentam atividade antibacteriana mais potente. A atividade analgésica mostrou que os compostos 1b, 4b e 5a apresentaram o melhor resultado usando métodos de placa quente em comparação com a droga padrão. Por outro lado, os compostos 1a, 4b e 5b deram boa atividade usando o método de contorção. **Conclusões:** Agentes analgésicos potentes, bons ou moderados e antibacterianos foram sintetizados usando reações químicas simples e de alto rendimento. As reações químicas incluem a síntese de agentes híbridos antibacterianos e analgésicos usando compostos de pirazolona.

**Palavras-chave:** Pirazolona, azoles, antibacteriano, analgésico, acoplamento molecular

## ABSTRACT

**Background:** 4-aminoantipyrine is one of the pyrazolone derivatives, it has been exposed to a large range of biological activities as an antimicrobial, analgesic, antiviral, anti-inflammatory, and anticancer compound. One of the important derivatives is the hybrid pyrazolone which includes two organic or inorganic drugs attached to give new pharmaceutical agents which may be the same or different activity from the original drugs. **Aim:** This research aimed to synthesize novel compounds derived from 4-aminoantipyrine and test their biological activity. **Methods:** Synthesis of 4-aminoantipyrine derivatives, which contain structurally two heterocyclic moieties, pyrazolone with oxadiazole, triazole, or tetrazole rings. The structures of the compounds were identified by <sup>1</sup>H-NMR and FT-IR spectroscopy. The *in vitro*, developed compounds were screened for their analgesic activity and antibacterial

activity against medically important gram (+) and gram (-) bacterial strains. **Results:** The antibacterial evaluation tests showed that some compounds gave good activity and others had no activity. The analgesic activity referred that the synthesized compounds had promising potency. The free binding energy (S) of the compounds with the protein 6B73 were -4.90 to -8.76 kcal/mol, whereas free energy (S) with the protein 5C1M gave -4.94 to -9.21 kcal/mol. **Discussion:** Among the tested compounds, it was found that compounds **1a**, **4b**, and **5a** had more potent antibacterial activity. The analgesic activity showed that compounds **1b**, **4b**, and **5a** gave the best activity using hot plate methods compared with the standard drug. On the other hand, compounds **1a**, **4b**, and **5b** gave good activity using the writhing test method. **Conclusions:** Potent, good, or moderate analgesic and antibacterial agents were synthesized using simple and high-yield chemical reactions. The chemical reactions include the synthesis of hybrid antibacterial and analgesic agents using pyrazolone compounds.

**Keywords:** Pyrazolone, azoles, antibacterial, analgesic, molecular docking.

## الخلاصة

**الخلفية:** يعتبر مركب 4-امينو انتيبيرين أحد مشتقات البيرازولون ، وقد اكتشف له مجموعة كبيرة من الأنشطة البيولوجية كمضاد للميكروبات ، ومسكن ، ومضاد للفيروسات ، ومضاد للالتهابات ، ومضاد للسرطان. أحد المشتقات الهامة هو البيرازولون الهجين الذي يحتوي على عقارين عضويين أو غير عضويين مرتبطين لإعطاء عوامل صيدلانية جديدة والتي قد تكون نفس النشاط أو مختلفة عن الأدوية الأصلية. **الهدف:** من هذا البحث هو تصنيع مركبات جديدة مشتقة من -امينو انتيبيرين واختبار نشاطها البيولوجي. **الطريقة:** تخليق مشتقات -امينو انتيبيرين التي تحتوي تركيباً على شقين غير متجانسين ، بيرازولون مع حلقات اوكساديازول ، أو ترازول ، أو ترازول. تم تحديد التركيب الكيميائي للمركبات بواسطة تحليل الرنين النووي المغناطيسي البروتوني ومطيافية الأشعة تحت الحمراء. في المختبر ، تم فحص المركبات المطورة لنشاطها المسكن ونشاطها المضاد للبكتيريا ضد صبغة الجرام (+) وضد صبغة الجرام (-) لبعض السلالات البكتيرية. **النتائج:** أظهرت اختبارات التقييم بمضادات البكتيريا أن بعض المركبات أعطت نشاطاً جيداً والبعض الآخر ليس له أي نشاط. يشير النشاط المسكن إلى أن المركبات المحضرة لها فاعلية واحدة. كانت طاقة الارتباط الحر (S) للمركبات التي تحتوي على البروتين B736 من -4.90 إلى -8.76 كيلوجول/مول ، بينما كانت الطاقة الحرة (S) مع 5C1M هي -4.94 إلى -9.21 كيلوجول/مول. **المناقشة:** من بين المركبات المختبرة ، وجد أن المركبات **a1** و **b4** و **a5** لها نشاط مضاد للجراثيم أقوى. أظهر النشاط المسكن أن المركبات **b1** ، **b4** ، **a5** أعطت أفضل فعالية باستخدام طرق اللوح الساخن مقارنة بالعقار القياسي. من ناحية أخرى ، أعطت المركبات **a1** و **b4** و **b5** نشاطاً جيداً باستخدام طريقة اختبار الانتواء. **الاستنتاجات:** تم تصنيع عوامل مسكنة ومضادة للجراثيم قوية أو جيدة أو معتدلة باستخدام تفاعلات كيميائية بسيطة وعالية المردود. تشمل التفاعلات الكيميائية تخليق العوامل الهجينة المضادة للبكتيريا والمسكنات باستخدام مركبات البيرازولون.

**الكلمات الدالة:** بايرازولون، ازولات، مضادات البكتيريا، مسكنات الألم، الارساء الجزيئي.

## 1. INTRODUCTION:

The increased biological activity of heterocyclic compounds and the fact that they allow for the creation of novel materials with distinctive features are two factors that contribute to the continual rise in interest in their synthesis. A biologically significant scaffold known as pyrazolone has been linked to numerous pharmacological activities, including antimicrobial (Verma *et al.*, 2021), anti-inflammatory (Mantzanidou *et al.*, 2021), analgesic (Bekhit *et al.*, 2022), antitubercular (Meta *et al.*, 2019), antioxidant (Silva *et al.*, 2018), and anticancer activities (Bennani *et al.*, 2020; Hassan *et al.*, 2021). Since they are members of a class of compounds with established medical chemistry applications, the synthesis of pyrazolone and its derivatives has attracted considerable interest from organic and medicinal chemists for many years.

Due to the widespread drug resistance, infectious diseases brought on by bacterial infections have emerged as a major public health issue. Bacterial and fungal infections play a role in morbidity and serious health issues produced globally (Ventola, 2015; Rayens & Norris, 2022).

Millions of people experience bacterial illnesses yearly (Mukherjee *et al.*, 2019). Winder and Collins published the first study on the isoniazid (INH) mechanism of action in 1970 (Vilchèze & Jacobs, 2019). Isoniazid derivatives can potentially make bacterial strains resistant (Al-Khattaf *et al.*, 2021), and isoniazid hybrids have been the subject of numerous antimicrobial agent attempts (Pienaar *et al.*, 2018; Panda *et al.*, 2019; Dackouo & Arama, 2019).

The idea of hybrid compounds, in which two or more pharmacophores are covalently connected to form a single entity, is appealing in medicinal chemistry (Pawelczyk *et al.*, 2018). The two components of the hybrid molecule may either exert dual pharmacological action by acting on distinct targets or work in opposition to each other to balance out undesirable effects. It is hypothesized that adding lipophilic moieties to the INH structure may boost the ability of the drug to penetrate tubercle bacilli and increase its anti-TB efficacy (Szumilak *et al.*, 2021).

An INH-pyrrole hybrid exhibits bactericidal activity against drug-sensitive and drug-resistant strains (Johansen *et al.*, 2021). Since isatin (2,3-dioxindole) provides a hydrophobic aromatic ring,

isatin-based compounds have remarkable anti-M. Tuberculosis capabilities and isatin-INH hybrids have drawn interest among the INH derivatives described thus far (Ding *et al.*, 2020; Abdel-Aziz *et al.*, 2017). Other research later showed that adding INH to isatin enhanced the antimycobacterial action of fresh compounds (Elsayed *et al.*, 2021).

The present study deals with synthesizing novel pyrazolone–isoniazid conjugates connected through sulfur linker using a molecular hybridization approach and investigating their biological properties against various microbial strains, including, *Staphylococcus aureus*, *Streptococcus*, *Escherichia coli*, and *Klebsiella pneumonia* mycobacteria and as analgesic agents.

## 2. MATERIALS AND METHODS:

The chemicals used were procured from the following companies, hydrazine hydrate, isonicotinic acid hydrazide, phenyl isothiocyanate, and sodium azide from Sigma-Aldrich Chemical Co. 4-aminoantipyrine, chloroacetyl chloride and 3-chloropropionyl chloride from Sunway Pharm (China). Absolute ethanol, dioxane, chloroform, and hydrochloric acid from Merck Ltd. Molar-Hintin agar from ALPHA (India). Uncorrected Barnstead electrothermal equipment in open capillaries was used to determine the physical characteristics of the produced compounds, particularly their melting point. Under UV light ( $\lambda = 254$  nm), thin layer analytical chromatography on silica gel 60 F254 aluminum sheets measuring 20 × 20 cm (Merck) was used to track the progress of the reaction and check the purity of the produced chemicals. <sup>1</sup>H-NMR spectrum of the compounds, tetramethylsilane (TMS) served as an internal standard, and dimethyl sulfoxide (DMSO-d<sub>6</sub>) served as the solvent and using a 500 MHz INOVA (Switzerland) spectrometer. In the Chemistry Department of the College of Science at Basrah University, the FT-IR spectra of each tested compound were measured as KBr disks using an FT-IR 8400S SHIMADZU (Japan) instrument. Using a CHN elemental analyzer flash EA 1112 series, synthetic substances underwent elemental microanalysis (CHN) (Thermo Finnigan).

### 2.1. Synthesis of compounds

#### 2.1.1 Synthesis of 2-chloro-N-(1,5-dimethyl-3-oxo-2-phenyl-2,3-dihydro-1H-pyrazol-4-yl)acetamide (1a) and 3-chloro-N-(1,5-dimethyl-3-oxo-2-phenyl-

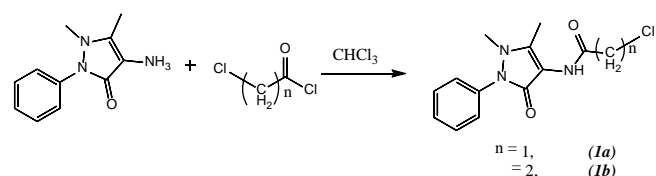
#### 2,3-dihydro-1H-pyrazol-4-yl)propenamide (1b)

The compounds **1a** and **1b** were synthesized according to the procedure in our paper (Mohammad *et al.*, 2021).

In a 100 mL round-bottomed flask, 15ml of chloroform, 2.03 g, 0.01 mole of 4-aminoantipyrine, and 0.132 g, 0.01 mole of anhydrous potassium carbonate was added. To this mixture, 0.01 mole of chloroacetyl chloride or 3-chloropropionyl chloride was added dropwise with stirring for 20 minutes. The reaction mixture was refluxed in a water bath at 60 °C for 3 hr. Next, chloroform was flashed to give the viscous solution, which was washed with (5% w/v, 35 mL) aqueous solution of sodium bicarbonate, the precipitate formed was filtered and dried, then recrystallized with ethanol.

**1a:** Pale yellow crystals, 55% yield, m. p. 190-193 °C, IR (KBr):  $\nu$  (cm<sup>-1</sup>) = 3190 (N-H), 3043 (C-H, aromatic), 2928, 2874 (C-H, aliphatic), 1693, 1639 (C=O, amide), 1558, 1489 (C=C), 1315, 1296 (C-N). <sup>1</sup>H NMR (DMSO-d<sub>6</sub>):  $\delta$  = 9.47 (s, 1H, NH), 7.52 -7.31 (m, 5H, Ar-H), 4.24 (s, 2H, CH<sub>2</sub>-Cl), 3.06 (s, 3H, N-CH<sub>3</sub>), 2.13 (s, 3H, C-CH<sub>3</sub>). Anal. Calc. (Found) for C<sub>13</sub>H<sub>14</sub>ClN<sub>3</sub>O<sub>2</sub> (279.72): C, 55.82 (55.89), H, 5.04 (5.17), N, 15.02 (14.66).

**1b:** Pale yellow crystals, 80% yield, m. p. 210-211 °C, IR (KBr):  $\nu$  (cm<sup>-1</sup>) = 3190 (N-H), 3009 (C-H, aromatic), 2889 (C-H, aliphatic), 1685, 1647 (C=O, amide), 1531, 1489 (C=C), 1315, 1199 (C-N). <sup>1</sup>H NMR (DMSO-d<sub>6</sub>):  $\delta$  = 9.27 (s, 1H, NH), 7.53 -7.31 (m, 5H, Ar-H), 3.86 (t, 2H,  $J = 6.2$  Hz, -CH<sub>2</sub>-Cl), 2.73 (t, 2H,  $J = 6.2$  Hz, -CH<sub>2</sub>-), 3.05 (s, 3H, N-CH<sub>3</sub>), 2.13 (s, 3H, C-CH<sub>3</sub>). Anal. Calc. (Found) for C<sub>14</sub>H<sub>16</sub>ClN<sub>3</sub>O<sub>2</sub> (293.75): C, 57.24 (57.62), H, 5.49 (5.13), N, 14.30 (14.70).



**Scheme 1.** Synthesis of compounds **1a** and **1b**

#### 2.1.2 Synthesis of 5-(pyridin-4-yl)-1,3,4-oxadiazole-2-thiol (2b)

In a mixture of 1.37g (0.1 moles) of isonicotinic acid hydrazide (INH) (**2a**), 0.9 mL (0.15 mole) of carbon disulfide, and 0.4g (0.1 moles) of sodium hydroxide (dissolved in the least amount of water) were added to a solution of 95% ethanol. The reaction mixture was heated at reflux for three hours until it no longer produced hydrogen sulfide.

The resulting mixture was diluted down and acidified with ice-cold diluted hydrochloric acid. The reaction mixture was filtered, water-washed, and recrystallized from ethanol for 30 minutes in an ice bath, as shown in Scheme 2 (Mohammed-Ali and Majeed, 2012).

**2a:** White crystals, 69% yield, m. p. 199-201 °C. IR (KBr):  $\nu$  (cm<sup>-1</sup>) = 3032 (C-H, aromatic), 2684 (S-H), 1597 (C=N, oxadiazole ring), 1489 (C=C), 1267, 1149 (C-O-C). <sup>1</sup>H NMR (DMSO-d<sub>6</sub>):  $\delta$  (ppm) = 7.81 (d, 2H, pyridine-*H*<sub>ortho</sub>), 8.81 (d, 2H, pyridine-*H*<sub>meta</sub>).

### 2.1.3 Synthesis of triazole

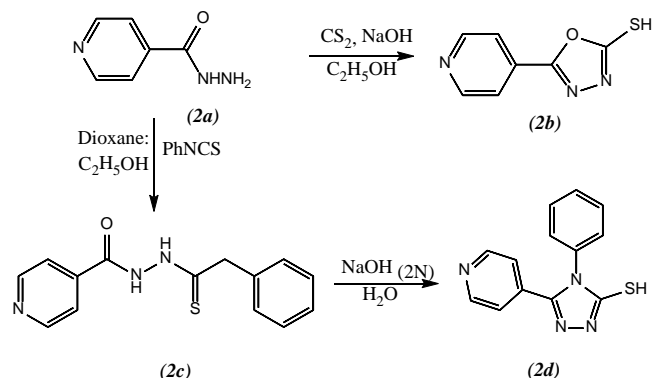
#### 2.1.3.1 Synthesis of thiosemicarbazide (2c)

At 60 °C, 1.19 mL (0.1 mole) of phenyl isothiocyanate was added to a mixture of 1.37g (0.1 mole) isonicotinic acid hydrazide **2a** in a cosolvent of dioxane:ethanol (4:1). The reaction mixture was agitated for 15 minutes at 60 °C and then for 1 hour at room temperature. The crystals were separated, filtered, and then dried at room temperature after being rinsed with cold ethanol, as shown in Scheme 2 (Alyahyaoy, 2019). Without additional purification, the products were utilized in the following phase.

#### 2.1.3.2 Synthesis of 4-phenyl-5-(pyridin-4-yl)-4H-1,2,4-triazole-3-thiol (2d)

Thiosemicarbazide **2c** and sodium hydroxide (0.005 mole) were dissolved in 50 mL of water and heated over reflux for two hours. After filtering, a cold solution of 2 M HCl was added to the yellow solution to lower the pH level to 4. Crystals were separated, filtered, and water-washed (Dhaif et al., 2019). The end products were dried at room temperature after being recrystallized from methanol, as shown in Scheme 2.

**2d:** Pale yellow crystals, 64.7% yield, m. p. 290-292 °C. IR (KBr):  $\nu$  (cm<sup>-1</sup>) = 3066, 3093 (C-H, aromatic), 2688 (S-H), 1566 (C=N, triazole ring), 1550 (C=C), 1288 (C-N). <sup>1</sup>H NMR (DMSO-d<sub>6</sub>):  $\delta$  (ppm) = 7.23 (d, 2H, pyridine-*H*<sub>ortho</sub>), 8.57 (d, 2H, pyridine-*H*<sub>meta</sub>), 7.41-7.56 (m, 5H, Ar-H phenyl-triazole).

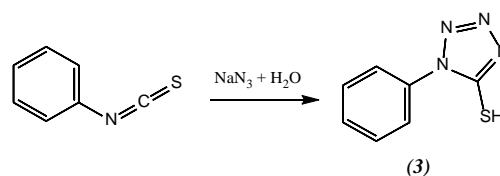


**Scheme 2.** Synthesis of compounds **2b** and **2d**

#### 2.1.4 Synthesis of 1-Phenyl-1,2,3,4-tetrazole-5-thiol (3)

The following materials were combined and refluxed for 4 hours: 150 ml of water, 5.98 ml (0.05 mole) of phenyl isothiocyanate, and 4.87 g (0.075 mole) of sodium azide. The mixture was filtered off after cooling to remove the unreacted phenyl isothiocyanate, and the filtrate was then extracted with diethyl ether. Litmus paper was used to measure the pH of the aqueous layer, which was then treated with hydrochloric acid to a pH of about 3. The precipitate was a white solid. After being dried and recrystallized with ethanol, the filtered crystals underwent a water wash, as shown in Scheme 3 (Abdul-Nabi & Jasim, 2014; AL-Hakiem, 2020).

**3:** White crystals, 91% yield, m. p. 153-155 °C. IR (KBr):  $\nu$  (cm<sup>-1</sup>) = 3034 (C-H, aromatic), 2713 (S-H), 1589 (C=N, oxadiazole ring), 1500 (C=C), 1454 (N=N), 1215 (C-N).



**Scheme 3.** Synthesis of compound **3**

#### 2.1.5 Synthesis of hybrid organic molecules 4a, 4b, 5a, and 5b

The compounds N-(1,5-dimethyl-3-oxo-2-phenyl-2,3-dihydro-1H-pyrazol-4-yl)-2-((4-phenyl-5-(pyridin-4-yl)-4H-1,2,4-triazol-3-yl)thio)acetamide **4a**, N-(1,5-dimethyl-3-oxo-2-phenyl-2,3-dihydro-1H-pyrazol-4-yl)-3-((5-(pyridin-4-yl)-1,3,4-oxadiazol-2-yl)thio)propenamide **4b**, N-(1,5-dimethyl-3-oxo-2-phenyl-2,3-dihydro-1H-pyrazol-4-yl)-2-((1-phenyl-1H-tetrazol-5-yl)thio)acetamide **5a** and N-(1,5-

dimethyl-3-oxo-2-phenyl-2,3-dihydro-1H-pyrazol-4-yl)-3-((1-phenyl-1H-tetrazol-5-yl)thio)propanamide **5b** were synthesized by the same procedure. (Othman *et al.*, 2019)

To a mixture containing 50 mL of absolute ethanol, 0.015 mole of the compounds **2b**, **2d**, or **3** and 0.018 mole of **1a** or **1b**, 0.02 mole of anhydrous sodium acetate were added. After being heated under reflux for three hours, the reaction mixture was allowed to cool and poured into 100 mL of ice-filled cold water. In order to recrystallize the solid, ethanol was collected and heated, as shown in Schemes 4 and 5.

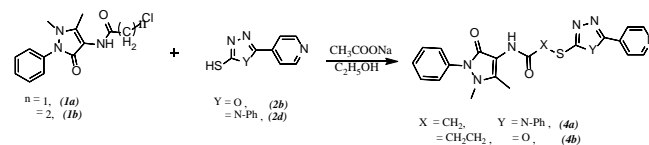
**4a**: Off-white crystals, 68.8% yield, m. p. 224-225 °C.  $\nu$  (cm<sup>-1</sup>) = 3321 (N-H), 3039 (C-H, aromatic), 2931 (C-H, aliphatic), 1678, 1643 (C=O, amide), 1600 (C=N), 1539 (C=C), 1188, 1148 (C-O, C-N). <sup>1</sup>H NMR (DMSO-d<sub>6</sub>):  $\delta$  (ppm) = 9.51 (s, 1H, NH), 7.51-7.62 (m, 5H, Ar-H phenyl-triazole), 7.30 (d, 2H, pyridine-*H*<sub>ortho</sub>), 8.56 (d, 2H, pyridine-*H*<sub>meta</sub>), 7.32-7.50 (m, 5H, Ar-H Phenyl-pyrazolone), 4.18 (s, 2H, -CH<sub>2</sub>-S), 3.04 (s, 3H, N-CH<sub>3</sub>), 2.11 (s, 3H, -CH<sub>3</sub>). Anal. Calc. (Found) for C<sub>26</sub>H<sub>23</sub>N<sub>7</sub>O<sub>2</sub>S (497.58): C, 62.76 (62.85), H, 4.66 (4.77), N, 19.71 (19.68).

**4b**: Off-white crystals, 69.1% yield, m. p. 210-211 °C.  $\nu$  (cm<sup>-1</sup>) = 3205 (N-H), 3032 (C-H, aromatic), 2889 (C-H, aliphatic), 1693, 1651 (C=O, amide), 1612 (C=N), 1531, 1452 (C=C), 1192, 1141 (C-N). <sup>1</sup>H NMR (DMSO-d<sub>6</sub>):  $\delta$  (ppm) = 9.25 (s, 1H, NH), 7.82 (d, 2H, pyridine-*H*<sub>ortho</sub>), 8.80 (d, 2H, pyridine-*H*<sub>meta</sub>), 7.31-7.50 (m, 5H, Ar-H Phenyl-pyrazolone), 3.56 (t, 2H, -CH<sub>2</sub>-S), 2.89 (t, 2H, -CH<sub>2</sub>-CH<sub>2</sub>-S), 3.05 (s, 3H, N-CH<sub>3</sub>), 2.13 (s, 3H, -CH<sub>3</sub>). Anal. Calc. (Found) for C<sub>21</sub>H<sub>20</sub>N<sub>6</sub>O<sub>3</sub>S (436.49): C, 57.79 (57.89), H, 4.52 (4.49), N, 19.25 (19.32).

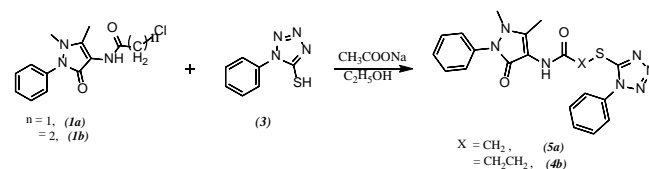
**5a**: Pale yellow crystals, 66.2% yield, m. p. 110-113 °C.  $\nu$  (cm<sup>-1</sup>) = 3301 (N-H), 3027 (C-H, aromatic), 2989 (C-H, aliphatic), 1678, 1658 (C=O, amide), 1613 (C=N), 1589, 1535 (C=C), 1199, 1095 (C-N). <sup>1</sup>H NMR (DMSO-d<sub>6</sub>):  $\delta$  (ppm) = 9.58 (s, 1H, NH), 7.67-7.73 (m, 5H, Ar-H phenyl-tetrazole), 7.31-7.53 (m, 5H, Ar-H Phenyl-pyrazolone), 4.36 (s, 2H, -CH<sub>2</sub>-S), 3.05 (s, 3H, N-CH<sub>3</sub>), 2.10 (s, 3H, -CH<sub>3</sub>). Anal. Calc. (Found) for C<sub>20</sub>H<sub>19</sub>N<sub>7</sub>O<sub>2</sub>S (421.48): C, 57.92 (57.84), H, 4.86 (4.80), N, 22.51 (22.46).

**5b**: Off-white crystals, 78.4% yield, m. p. 156-158 °C.  $\nu$  (cm<sup>-1</sup>) = 3178 (N-H), 3020 (C-H, aromatic), 2931 (C-H, aliphatic), 1681, 1647 (C=O, amide), 1620 (C=N), 1589, 1531 (C=C), 1203, 1145 (C-N). <sup>1</sup>H NMR (DMSO-d<sub>6</sub>):  $\delta$  (ppm) = 9.23 (s, 1H, NH), 7.65-7.67 (m, 5H, Ar-H phenyl-tetrazole), 7.31-7.52 (m, 5H, Ar-H Phenyl-

pyrazolone), 3.67 (t, 2H, -CH<sub>2</sub>-S), 2.86 (t, 2H, -CH<sub>2</sub>-CH<sub>2</sub>-S), 3.04 (s, 3H, N-CH<sub>3</sub>), 2.06 (s, 3H, -CH<sub>3</sub>). Anal. Calc. (Found) for C<sub>21</sub>H<sub>21</sub>N<sub>7</sub>O<sub>2</sub>S (435.51): C, 56.99 (57.11), H, 4.54 (4.52), N, 23.26 (23.16).



**Scheme 4.** Synthesis of compounds **4a** and **4b**



**Scheme 5.** Synthesis of compounds **5a** and **5b**

## 2.2 Antibacterial Activity Evaluation

For evaluating in vitro antibacterial, Gram-positive bacteria (*S. aureus* and *Streptococcus*) and Gram-negative bacteria (*E. coli* and *Klebsiella pneumonia*) were used by disc diffusion method. Dimethyl sulfoxide (DMSO) was used to dissolve the compounds in solutions at concentrations of 1000, 500, 250, 125, and 50 g/ml. Mueller-Hinton Agar in the 20–30 ml volume was put into the 100 mm Petri plate. Whatman No. 4 (6 mm) diameter; impregnated with solutions of the chemicals under investigation. After that, the disc was placed on the medium's surface utilizing microorganisms. Twenty-four hours of incubation on Petri dishes at 37 °C. The antibacterial efficacy was calculated by measuring the diameter of the inhibitory zone in mm. (Mohammed & Mustafa, 2020; Fouad *et al.*, 2021).

## 2.3 Evaluation of Analgesic Activity

### 2.3.1 Writhing Test

Six albino mice were placed in each of the fourteen groups of albino mice. Animals that had been fasting overnight received the following care: Group 1 of mice was treated with (10 mL/kg) of vehicle (olive oil) and served as the control group, and Group 2 of mice was treated with 10 mg/kg of paracetamol and served as a standard group, while groups (3–14) were received 10 mg/kg of tested compounds. Every dosage of the compounds, paracetamol, and experimental drugs was administered orally via gastric gavage. To produce the nociception condition, mice in all groups received 10 mL/kg of a 1% v/v acetic acid solution intraperitoneally (i.p.) after 1 hour (pain).

The number of observed writhings in each mouse was tallied for 15 minutes, starting 5 minutes after the administration of acetic acid. The following method, Equation 1, was used to compute the percentage inhibition (I%) of writhing (abdominal constrictions), which was used to assess the analgesic potency:

$$\text{Inhibition\% (I\%)} = \left( \frac{N_c - N_t}{N_c} \right) \times 100 \quad (\text{Eq. 1})$$

Where  $N_c$  is the average of writhing numbers in the control group and  $N_t$  is the average of writhing numbers in the tested groups (Yimer *et al.*, 2020).

### 2.3.2 Hot Plate Test

Swiss albino mice of both sexes were divided into fourteen groups for this experiment, with six mice in each group. The mice were given the following care after an overnight fast: As a control group, group 1 of mice received 10 mL/kg of vehicle (olive oil), while group 2 of mice received 10 mg/kg of paracetamol as the standard group, and groups 3 through 14 of mice received 10 mg/kg of the test compounds orally. Mice were placed inside a glass cylinder on a well-controlled hot plate that was kept at a temperature of 55°C after an hour of all oral treatments. The time interval between the placement of the mice on the hot plate surface and the occurrence of fore or hind paw licking or jumping was noted as reaction time and was calculated using Equation 2.

$$\text{Inhibition\% (I\%)} = \left( \frac{T_t - T_c}{T_c} \right) \times 100 \quad (\text{Eq. 2})$$

Where  $T_t$  is the average reaction time in the tested group and  $T_c$  is the average reaction time in the control groups. To prevent paw injury, it has been considered that the cutoff period should not last more than 20 sec (Santenna *et al.*, 2019).

### 2.4 Docking studies

All compounds were projected using ChemDraw Software 2016. All water molecules and ligands were removed during molecular docking of the produced compounds **1a**, **1b**, **2b**, **2d**, **3**, **4a**, **4b**, **5a**, and **5b** using MOE 2015 v10. The crystal Structure of a nanobody-stabilized active state of the kappa-opioid receptor (protein ID: 6B73) and the crystal structure of the active mu-opioid receptor (proteins ID: 5C1M) were obtained from the RCSB protein data bank.

## 3. RESULTS AND DISCUSSION:

### 3.1. Results

In this study, it was synthesized some derivatives of 4-aminoantipyrine and tested for their antibacterial activity against selected bacteria, as well as their analgesic activities. Finally, we theoretically analyzed their properties regarding their molecular docking properties with selected protein sites. All the compounds were synthesized with good yield in pure form. Synthesized compounds were identified using melting point, and spectroscopic methods include FT-IR and <sup>1</sup>H-NMR techniques.

Synthesized compounds were evaluated for antibacterial and analgesic activities. The results of the antibacterial potential of compounds are presented in Table 1, and the results gave a clear view that the synthesized compounds exhibited different values of potency. We noted that compounds **1a**, **1b**, **4b**, and **5a** gave an inhibition zone against all types of bacteria at the highest concentration (1000 µg/mL), whereas compound **5b** exhibited activity against three bacteria except Streptococcus, and finally, compound **4a** gave an activity against only Gram-negative bacteria.

The analgesic activity of the compounds **1a**, **1b**, **4a**, **4b**, **5a**, and **5b** was evaluated in mice using the analgesia hot plate and writhing test methods compared with paracetamol as a standard drug. Table 2 shows the analgesic activity depending on the reaction time and inhibition% of the synthesized compounds and standard drugs by hot plate method, while Table shows the number of writhing and inhibition% of the synthesized compounds and standard drugs by the writhing method. Figure 1 shows the analgesic activity of the compounds using two methods.

Molecular docking analysis is the most effective way of determining how a target protein interacts with an inhibitory substance (Attique *et al.*, 2019; Arjmand *et al.*, 2022; Durhan *et al.*, 2022). Docking investigations were performed using the software MOE (2015.10). The 3D crystallographic structure of the protein was downloaded from the Protein Data Bank website (www.rcsb.org) (PDB ID: 6B73 and ID: 5C1M). All compounds were represented by their 2D structures on ChemDraw Ultra 16.0.

The covalent docking of the synthesized compounds into the largest pocket of the kappa-opioid receptor (6B73) and mu-opioid receptor (5C1M) was simulated, and the docking scores

results are shown in Table 4. Tables 5 and 6 display the findings for just the substances that produced reliable molecular docking scores. The best simulation of the synthesized compounds with two types of protein was the final derivatives **4a**, **4b**, **5a**, and **5b**, which showed greater value S scores, as shown in Figures 1 and 2.

## 3.2. Discussions

### 3.2.1. Chemistry

Heating of isonicotinic acid hydrazide with carbon disulfide in the presence of an alcoholic alkaline medium gave sodium xanthate salt, which lost the hydrogen sulfide to form sodium oxadiazole ion, which was converted to oxadiazole thiol **2b** in an acidic medium. IR spectrum showed the medium absorption band at  $2684\text{ cm}^{-1}$  attributed to the stretching vibration of the S-H bond (Hudson and Gerakines, 2018), and the medium band at  $1597\text{ cm}^{-1}$  referred to the stretching vibration of C=N of the oxadiazole ring. In addition, the  $^1\text{H-NMR}$  gave aromatic protons of the pyridine ring at 7.81 and 8.81 ppm, attributed to ortho and meta protons as doublet, respectively.

Two steps synthesized the triazole compound **2d**, and the first included the synthesis of the intermediate thiosemicarbazide **2c** by mild heating of isonicotinic acid hydrazide and phenyl iso-thiocyanate in dioxane:ethanol cosolvent. In the second step, the white crystals of **2c**, which separated, were subjected to cyclization in an aqueous alkaline medium. After treatment with an acidic solution, pale-yellow precipitation was formed. IR spectrum of **2d** gave a medium band at  $2688\text{ cm}^{-1}$  which attributed to the stretching vibration of the S-H band, and the medium band at  $1688\text{ cm}^{-1}$  referred to the stretching vibration of the C=N bond of the triazole ring (Salinas-Torres *et al.*, 2022). In addition,  $^1\text{H-NMR}$  gave doublet signals aromatic pyridine protons at 7.23 and 8.57 ppm, another multiplet signal in the range 7.41-7.56 ppm related to protons of phenyl ring attached to triazole ring.

The synthesis of compound 1-phenyl-1,2,3,4-tetrazole-5-thiol **3** included cyclization of phenyl iso-thiocyanate with sodium azide in an aqueous solution to give white crystals with a good yield. The final product identified by IR spectroscopy gave a medium absorption band at  $2713\text{ cm}^{-1}$  attributed to the stretching vibration of the S-H band and a strong band at  $1454\text{ cm}^{-1}$  referred to as N=N stretching vibration.

The final compounds **4a**, **4b**, **5a**, and **5b** were synthesized by sulfur nucleophilic

substitution (an attack by  $\text{S}^-$ ) at the carbon atom attached to chloride of **1a** and **1b**, and the mechanism of the reaction is according to  $\text{S}_{\text{N}}2$ . The IR spectra of the products characterized by the lack of the S-H band and appearing in the medium-strong bands at the range  $1678\text{-}1693\text{ cm}^{-1}$  and  $1643\text{-}1658\text{ cm}^{-1}$  attributed to stretching vibration of carbonyl open and cyclic amide groups (Balan *et al.*, 2019).  $^1\text{H-NMR}$  of all compounds showed the following signals, singlet signal at 9.23-9.58 ppm related to one proton of the H-N-C=O group, characteristic high field singlet signals at 3.04-3.05 and 2.06-2.13 ppm attributed to three protons of methyl groups attached to nitrogen and carbon atoms, respectively, of pyrazolone ring. The compounds **4a** and **5a** gave singlet signals at 4.18 and 4.36 ppm, respectively, related to two protons of methylene groups attached to the sulfur atom, while the compounds **4b** and **5b** gave triplet signals at 3.56 and 3.67 ppm attributed to methylene protons attached to sulfur atoms and coupled with another proton of methylene group with  $J=6.7\text{ Hz}$ .

### 3.2.2 Antibacterial activity

The compounds **1a**, **1b**, **4a**, **4b**, **5a**, and **5b** were tested for their antibacterial activity against Gram-negative bacteria (*Escherichia coli* and *Klebsiella pneumonia*) and Gram-positive bacteria (*Staphylococcus aureus* and *Streptococcus*) employing the filter paper disc diffusion method, and the inhibition zone diameter was measured after 24 hr. The preliminary results indicated that some compounds were active against the tested bacteria, as shown in Table 1.

Compound **1a** gave the best activity (17 mm) against *Streptococcus* at  $1000\text{ }\mu\text{g/mL}$  as compared with other compounds, while mild activity as compared with standard drug (amoxicillin) at the same concentration. The compounds **1a**, **4b**, and **5a** showed good activity against all bacterial strains under investigation at the highest concentration ( $1000\text{ }\mu\text{g/mL}$ ). All compounds gave an inhibition zone in the range (7-9) mm against *Escherichia coli*. In contrast, some compounds gave an inhibition zone from no inhibition to 12 mm against *Klebsiella pneumonia* at the highest concentration. The compound **4a** gave weaker activity, which showed no inhibition against Gram-positive bacteria while giving inhibition zone 9 and 7 mm against *Escherichia coli* and *Klebsiella pneumonia*, respectively.

### 3.2.3. Analgesic activity

The results showed that compounds **1b**, **4b**, and **5a** gave the best activity (40%, 45%, and 51%, respectively) compared with other compounds. On the other hand, the synthesized compound **4a** gave moderate activity (32%) as compared with the standard drug.

The good activity of compounds **4b** and **5a** may be attributed to the chemical structure of the two types of compounds. It was observed that the presence of the compound fragment that contains the heterocyclic rings (oxadiazole and tetrazole) in these compounds gave better activity, which may be attributed to the presence of the heterocyclic rings that affect the physicochemical and pharmacokinetic properties of the entire compound (Hardjono *et al.*, 2017; Mazák *et al.*, 2019).

The results showed that compounds **1a**, **4b**, and **5b** gave good activity (68%, 52%, and 47%, respectively) compared with other compounds. On the other hand, the synthesized compounds **1b** and **4a** gave moderate activity (30% and 30%) as compared with the standard drug. Finally, it was noted that compound **4b** gave the best activity in every two methods as compared with the standard drug, as shown in Figure 1.

#### 3.2.4. Molecular Docking Studies

The results showed that compounds favorable docking scores ranging from -4.90 to -8.76 kcal/mol and RMSD values in the range 1.05 to 2.31 Å with 6B73, whereas these compounds gave affinity in the range -4.94 to -9.20 kcal/mol and RMSD values 1.10 to 2.34 Å with the 5C1M protein. Compound **5b** gave the best affinity with 6B73 protein at -8.76 kcal/mol, whereas compound **4b** showed the best affinity with 5C1M protein (-9.20 kcal/mol).

According to Table 1, compound **5b** gave the highest docking scores of -8.76 kcal/mol and RMSD value 1.91 Å, which gave a good inhibitory potential of 47% in the writhing method. Compound **5b** docked with a binding affinity of -46.85 kcal/mol, which is the highest compared with the others, and interacted with LEU 212. Compound **4a** docked with a good binding affinity of -46.83 kcal/mol and interacted with LEU 212, LYS 227, and TYR 139. Compound **4b** docked with a binding affinity of -45.79 kcal/mol and interacted with CYS 210, GLN 115, and GLN 115.

Compound **4b**, which docked with the highest binding affinity of -48.66 kcal/mol when compared to the other compounds and interacted with MET 151, LYS 303, and HIS 54, had the

highest docking scores of -9.21 kcal/mol and RMSD value 1.34 Å, as shown in Table 2. With a binding affinity of about -46.52 kcal/mol, compound **5b** docked and interacted with LYS 233 and SER 53. With a binding affinity of about -46.21 kcal/mol, compound **5a** docked and interacted with HIS 54 and SER 53.

## 4. CONCLUSIONS:

The present study describes the synthesis of pyrazolone compounds **4a**, **4b**, **5a**, and **5b** by reaction of 4-aminoantipyrine derivatives **1a** and **1b** and some synthesized heterocyclic compounds (oxadiazole; **2b**, triazole; **2d**, and tetrazole; **3**). The results of the antimicrobial evaluation revealed that the activity of the compounds was between good and moderate. In contrast, the analgesic activity gave a clear view of the potency of some of the synthesized compounds as analgesic agents. Furthermore, according to the molecular docking studies, the final compounds (**4a**, **4b**, **5a**, and **5b**) gave very good binding affinity coordinated with the largest site proteins (6B73 and 5C1M) compared with other synthesized compounds under investigation.

## 5. DECLARATIONS

### 5.1. Study Limitations

Identification of the synthesized compounds must be done in private laboratories out of Iraq.

### 5.2. Funding source

This work was financially supported by the Authors.

### 5.3. Competing Interests

The authors declare no conflicts of interest.

### 5.4. Open Access

This article is licensed under a Creative Commons Attribution 4.0 (CC BY 4.0) International License, which permits use, sharing, adaptation, distribution, and reproduction in any medium or format, as long as you give appropriate credit to the original author(s) and the source, provide a link to the Creative Commons license, and indicate if changes were made. The images or other third-party material in this article are included in the article's Creative Commons license unless indicated otherwise in a credit line to the material. If material is not included in the article's Creative Commons license and your intended use is not



permitted by statutory regulation or exceeds the permitted use, you will need to obtain permission directly from the copyright holder. To view a copy of this license, visit <http://creativecommons.org/licenses/by/4.0/>.

## 6. HUMAN AND ANIMAL-RELATED STUDIES

### 6.1. Ethical Approval

All of the dealing procedures with animals described in this study were authorized by the Animal Ethics Committee, University of Basrah, Iraq (No. 2013/32).

## 7. REFERENCES:

1. Verma, R., Verma, S. K., Rakesh, K. P., Girish, Y. R., Ashrafizadeh, M., Kumar, K. S. S., & Rangappa, K. S. (2021). Pyrazole-based analogs as potential antibacterial agents against methicillin-resistance staphylococcus aureus (MRSA) and its SAR elucidation. *European journal of medicinal chemistry*, 212, 113134. <https://doi.org/10.1016/j.ejmech.2020.113134>
2. Mantzanidou, M., Pontiki, E., & Hadjipavlou-Litina, D. (2021). Pyrazoles and pyrazolines as anti-inflammatory agents. *Molecules*, 26(11), 3439. <https://doi.org/10.3390/molecules26113439>
3. Bekhit, A. A., Nasralla, S. N., El-Agroudy, E. J., Hamouda, N., Abd El-Fattah, A., Bekhit, S. A., ... & Ibrahim, T. M. (2022). Investigation of the anti-inflammatory and analgesic activities of promising pyrazole derivative. *European Journal of Pharmaceutical Sciences*, 168, 106080. <https://doi.org/10.1016/j.ejps.2021.106080>
4. Meta, E., Brullo, C., Tonelli, M., Franzblau, S. G., Wang, Y., Ma, R., ... & Bruno, O. (2019). Pyrazole and imidazo [1, 2-b] pyrazole derivatives as new potential anti-tuberculosis agents. *Medicinal Chemistry*, 15(1), 17-27. <https://doi.org/10.2174/1573406414666180524084023>
5. Silva, V. L., Elguero, J., & Silva, A. M. (2018). Current progress on antioxidants incorporating the pyrazole core. *European journal of medicinal chemistry*, 156, 394-429. <https://doi.org/10.1016/j.ejmech.2018.07.07>
6. Bennani, F. E., Doudach, L., Cherrah, Y., Ramli, Y., Karrouchi, K., & Faouzi, M. E. A. (2020). Overview of recent developments of pyrazole derivatives as an anticancer agent in different cell line. *Bioorganic Chemistry*, 97, 103470. <https://doi.org/10.1016/j.bioorg.2019.103470>
7. Hassan, A. S., Moustafa, G. O., Awad, H. M., Nossier, E. S., & Mady, M. F. (2021). Design, synthesis, anticancer evaluation, enzymatic assays, and a molecular modeling study of novel pyrazole-indole hybrids. *ACS omega*, 6(18), 12361-12374. <https://doi.org/10.1021/acsomega.1c01604>
8. Ventola, C. L. (2015). The antibiotic resistance crisis: part 1: causes and threats. *Pharmacy and therapeutics*, 40(4), 277.
9. Rayens, E., & Norris, K. A. (2022, January). Prevalence and healthcare burden of fungal infections in the United States, 2018. In *Open forum infectious diseases* (Vol. 9, No. 1, p. ofab593). US: Oxford University Press. <https://doi.org/10.1093/ofid/ofab593>
10. Mukherjee, S., Anderson, C. M., Mosci, R. E., Newton, D. W., Lephart, P., Salimnia, H., ... & Manning, S. D. (2019). Increasing frequencies of antibiotic resistant nontyphoidal Salmonella infections in Michigan and risk factors for disease. *Frontiers in medicine*, 250. <https://doi.org/10.3389/fmed.2019.00250>
11. Vilch eze, C., & Jacobs Jr, W. R. (2019). The isoniazid paradigm of killing, resistance, and persistence in Mycobacterium tuberculosis. *Journal of molecular biology*, 431(18), 3450-3461. <https://doi.org/10.1016/j.jmb.2019.02.016>
12. Al-Khattaf, F. S., Mani, A., Hatamleh, A. A., & Akbar, I. (2021). Antimicrobial and cytotoxic activities of isoniazid connected menthone derivatives and their investigation of clinical pathogens causing infectious disease. *Journal of Infection and Public Health*, 14(4), 533-542. <https://doi.org/10.1016/j.jiph.2020.12.033>
13. Pienaar, E., Linderman, J. J., & Kirschner, D. E. (2018). Emergence and selection of isoniazid and rifampin resistance in tuberculosis granulomas. *PLoS One*, 13(5), e0196322. <https://doi.org/10.1371/journal.pone.0196322>
14. Panda, S. S., Girgis, A. S., Mishra, B. B., Elagawany, M., Devarapalli, V., Littlefield,

- W. F., ... & Bokhtia, R. M. (2019). Synthesis, computational studies, antimycobacterial and antibacterial properties of pyrazinoic acid–isoniazid hybrid conjugates. *RSC advances*, 9(35), 20450-20462. <https://doi.org/10.1039/c9ra03380g>
15. Dackouo, B., & Arama, D. P. (2019). Systematic Review of New Trends in Antitubercular Synthesis and Analysis. *Journal of Materials Science and Chemical Engineering*, 7(01), 1. <https://doi.org/10.4236/msce.2019.71001>
  16. Pawełczyk, A., Sowa-Kasprzak, K., Olender, D., & Zaprutko, L. (2018). Molecular consortia—Various structural and synthetic concepts for more effective therapeutics synthesis. *International journal of molecular sciences*, 19(4), 1104. <https://doi.org/10.3390/ijms19041104>
  17. Szumilak, M., Wiktorowska-Owczarek, A., & Stanczak, A. (2021). Hybrid drugs—a strategy for overcoming anticancer drug resistance? *Molecules*, 26(9), 2601. <https://doi.org/10.3390/molecules26092601>
  18. Johansen, M. D., Shalini, Kumar, S., Raynaud, C., Quan, D. H., Britton, W. J., ... & Kremer, L. (2021). Biological and biochemical evaluation of isatin-isoniazid hybrids as bactericidal candidates against mycobacterium tuberculosis. *Antimicrobial agents and chemotherapy*, 65(8), e00011-21. <https://doi.org/10.1128/AAC.00011-21>
  19. Ding, Z., Zhou, M., & Zeng, C. (2020). Recent advances in isatin hybrids as potential anticancer agents. *Archiv der Pharmazie*, 353(3), 1900367. <https://doi.org/10.1002/ardp.201900367>
  20. Abdel-Aziz, H. A., Eldehna, W. M., Keeton, A. B., Piazza, G. A., Kadi, A. A., Attwa, M. W., ... & Attia, M. I. (2017). Isatin-benzoazine molecular hybrids as potential antiproliferative agents: synthesis and in vitro pharmacological profiling. *Drug Design, Development and Therapy*, 11, 2333. <https://doi.org/10.2147/DDDT.S140164>
  21. Elsayed, Z. M., Eldehna, W. M., Abdel-Aziz, M. M., El Hassab, M. A., Elkaeed, E. B., Al-Warhi, T., ... & Mohammed, E. R. (2021). Development of novel isatin–nicotinohydrazide hybrids with potent activity against susceptible/resistant Mycobacterium tuberculosis and bronchitis causing–bacteria. *Journal of enzyme inhibition and medicinal chemistry*, 36(1), 384-392. <https://doi.org/10.1080/14756366.2020.1868450>
  22. Mohammad, A. E., Muhammad-Ali, M. A., Hameed, B. J., & Shaheed, D. Q. (2021). Design, synthesis, and characterization of some novel 4-aminoantipyrine derivatives and evaluation of their activity as analgesic agents. *Acta Poloniae Pharmaceutica*, 78(5), 627-634. <https://doi.org/10.32383/appdr/144130>
  23. Mohammed-Ali, M. A., & Majeed, N. N. (2012). Synthesis, characterization and study of antibacterial and antifungal activities of some 1, 3, 4-oxadiazole compounds. *J. Chem. Pharm. Res*, 4, 315-321.
  24. Alyahyaoy, H. A. (2019). Synthesis, characterization and antibacterial evaluation of new 1, 2, 4-triazole-3-thiol derivatives. *International Journal of Green Pharmacy (IJGP)*, 13(3). <https://doi.org/10.22377/ijgp.v13i3.2600>
  25. Dhaif, H. K., Jasim, E. Q., Muhajjar, Z. A., & Shanta, A. A. (2019). Corrosion Inhibition of Mild-Steel in 0.5 M HCl using some prepared 1, 2, 3-Triazoles Derivatives. *Mediterranean Journal of Chemistry*, 9(4), 290-304. <https://doi.org/10.13171/mjc941911101065hkd>
  26. Abdul-Nabi, A. S., & Jasim, E. Q. (2014). Synthesis, Characterization and study of some tetrazole compounds as new corrosion inhibitors for C-steel in 0.5 M HCl solution. *International Journal of Engineering Research*, 3(10), 613-617.
  27. AL-Hakiem MM. (2020). Synthesis, Characterization and Biological Evaluation of Some Sulfa Drug Derivatives. *MSc Thesis, University of Basrah*.
  28. Othman, A. A., Kihel, M., & Amara, S. (2019). 1, 3, 4-Oxadiazole, 1, 3, 4-thiadiazole and 1, 2, 4-triazole derivatives as potential antibacterial agents. *Arabian Journal of Chemistry*, 12(7), 1660-1675. <https://doi.org/10.1016/j.arabjc.2014.09.003>
  29. Mohammed, E. T., & Mustafa, Y. F. (2020). Coumarins from Red Delicious apple seeds: Extraction, phytochemical analysis, and evaluation as antimicrobial agents. *Systematic Reviews in Pharmacy*, 11(2), 64-70. DOI: <https://doi.org/10.5530/srp.2020.2.11>
  30. Fouad, S. A., El-Gendey, M. S., Ahmed, E. M., Hessein, S. A., Ammar, Y. A., & Zaki,

- Y. H. (2021). Convenient Synthesis of Some New Thiophene, Pyrazole, and Thiazole Derivatives Bearing Biologically Active Sulfonyl Guanidine Moiety. *Polycyclic Aromatic Compounds*, 1-19.  
<https://doi.org/10.1080/10406638.2021.1988999>
31. Yimer, T., Birru, E. M., Adugna, M., Geta, M., & Emiru, Y. K. (2020). Evaluation of analgesic and anti-inflammatory activities of 80% methanol root extract of *Echinops kebericho* M.(Asteraceae). *Journal of Inflammation Research*, 13, 647.  
<https://doi.org/10.2147/JIR.S267154>
  32. Santenna, C., Kumar, S., Balakrishnan, S., Jhaj, R., & Ahmed, S. N. (2019). A comparative experimental study of analgesic activity of a novel non-steroidal anti-inflammatory molecule–zaltoprofen, and a standard drug–piroxicam, using murine models. *Journal of Experimental Pharmacology*, 11, 85.  
<https://doi.org/10.2147/JEP.S212988>
  33. Attique, S. A., Hassan, M., Usman, M., Atif, R. M., Mahboob, S., Al-Ghanim, K. A., ... & Nawaz, M. Z. (2019). A molecular docking approach to evaluate the pharmacological properties of natural and synthetic treatment candidates for use against hypertension. *International journal of environmental research and public health*, 16(6), 923.  
<https://doi.org/10.3390/ijerph16060923>
  34. Arjmand, B., Hamidpour, S. K., Alavi-Moghadam, S., Yavari, H., Shahbazbadr, A., Tavirani, M. R., ... & Larijani, B. (2022). Molecular Docking as a Therapeutic Approach for Targeting Cancer Stem Cell Metabolic Processes. *Frontiers in pharmacology*, 13.  
<https://doi.org/10.3389/fphar.2022.768556>
  35. Durhan, B., Yalçın, E., Çavuşoğlu, K., & Acar, A. (2022). Molecular docking assisted biological functions and phytochemical screening of *Amaranthus lividus* L. extract. *Scientific reports*, 12(1), 1-16.  
<https://doi.org/10.1038/s41598-022-08421-8>
  36. Hudson, R. L., & Gerakines, P. A. (2018). Infrared spectra and interstellar sulfur: New laboratory results for H<sub>2</sub>S and four malodorous thiol ices. *The Astrophysical Journal*, 867(2), 138.  
<https://doi.org/10.3847/1538-4357/aae52a>
  37. Salinas-Torres, A., Portilla, J., Rojas, H., Becerra, D., & Castillo, J. C. (2022). Synthesis, Spectroscopic Analysis, and In Vitro Anticancer Evaluation of 2-(Phenylsulfonyl)-2H-1, 2, 3-triazole. *Molbank*, 2022(2), M1387.  
<https://doi.org/10.3390/M1387>
  38. Balan, V., Mihai, C. T., Cojocaru, F. D., Uritu, C. M., Dodi, G., Botezat, D., & Gardikiotis, I. (2019). Vibrational spectroscopy fingerprinting in medicine: from molecular to clinical practice. *Materials*, 12(18), 2884.  
[tps://doi.org/10.3390/ma12182884](https://doi.org/10.3390/ma12182884)
  39. Hardjono, S., Siswandono, S., & Andayani, R. (2017). Evaluation of N-benzoylthiourea derivatives as possible analgesic agents by predicting their physicochemical and pharmacokinetic properties, toxicity, and analgesic activity. *Indonesian Journal of Biotechnology*, 22(2), 76-85.  
<https://doi.org/10.22146/ijbiotech.27171>
  40. Mazák, K., Noszál, B., & Hosztafi, S. (2019). Advances in the physicochemical profiling of opioid compounds of therapeutic interest. *ChemistryOpen*, 8(7), 879-887.  
<https://doi.org/10.1002/open.201900115>

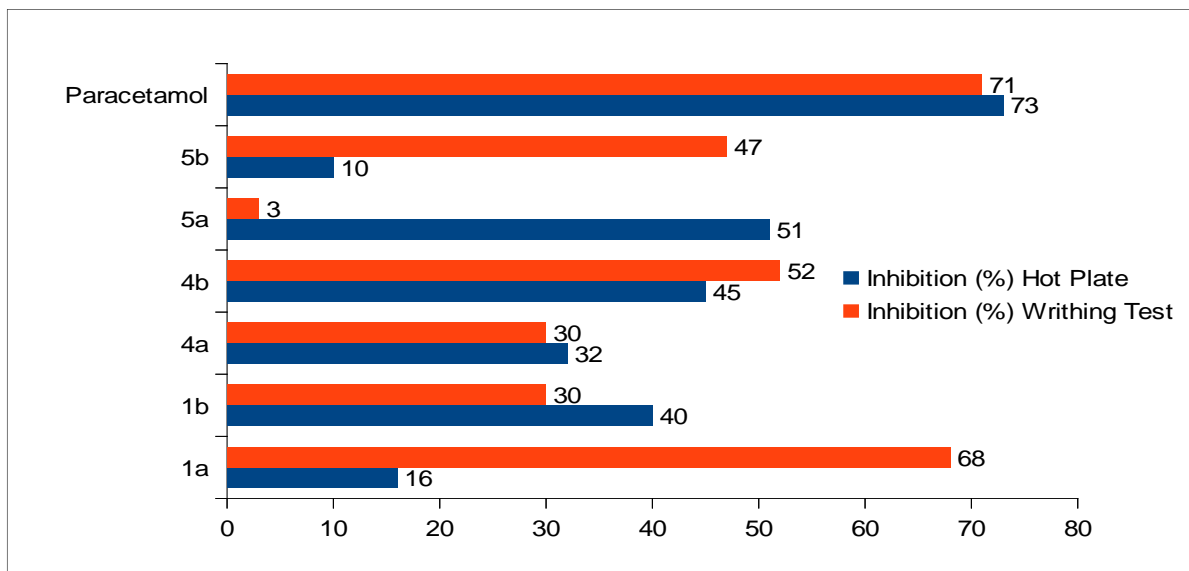


**Figure 1.** Analgesic activity of the compounds using hot plate and writhing test methods

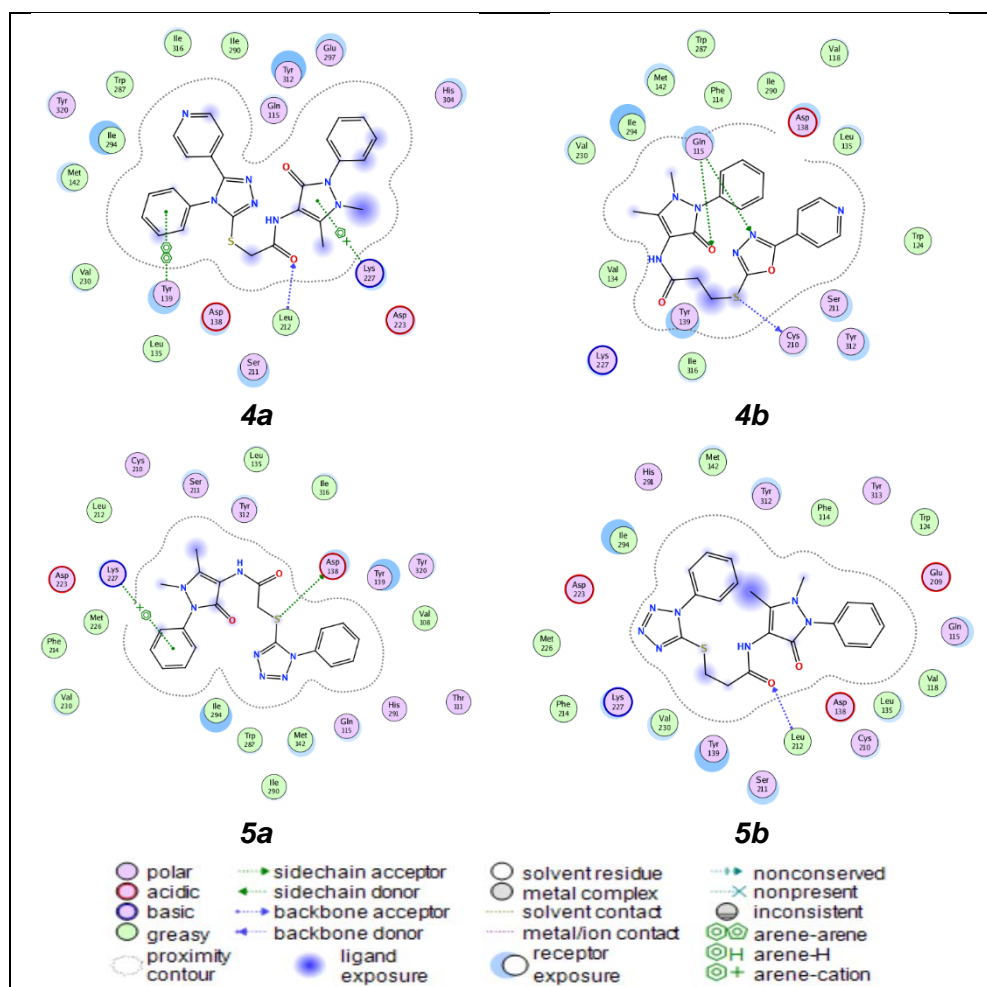


**Figure 2.** 2D binding affinity of the compounds with 6B73

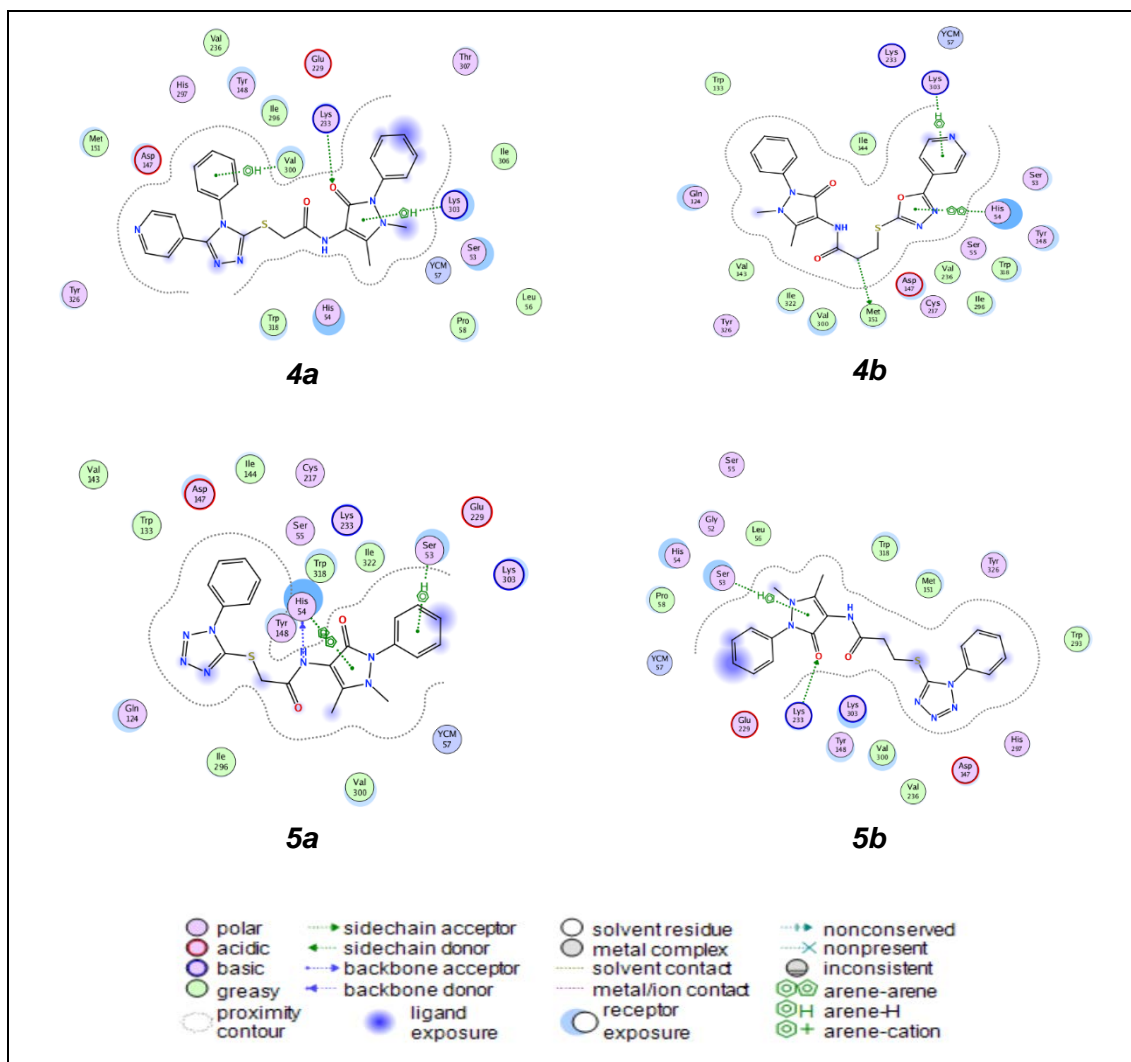


**Figure 3.** 2D binding affinity of the compounds with 5C1M

**Table 1.** Inhibition zone of the synthesized compounds against the tested bacteria at different concentrations

Compound	Conc. (µg/ml)	Inhibition zone (mm)			
		<i>S. aureus</i>	<i>Streptococcus</i>	<i>E.coli</i>	<i>Klebsiella pneumonia</i>
1a	1000	10	17	9	8
	500	10	15	7	8
	250	8	15	7	NI
	125	7	10	NI	NI
	50	7	8	NI	NI
1b	1000	10	10	7	NI
	500	9	7	7	NI
	250	7	7	NI	NI
	125	NI	NI	NI	NI
	50	NI	NI	NI	NI
4b	1000	10	9	8	8
	500	9	9	8	7
	250	7	7	7	7
	125	7	NI	NI	NI
	50	NI	NI	NI	NI
4a	1000	NI	NI	9	7
	500	NI	NI	7	NI
	250	NI	NI	7	NI
	125	NI	NI	NI	NI
	50	NI	NI	NI	NI
5a	1000	11	9	9	12
	500	8	7	7	9
	250	7	NI	7	7
	125	NI	NI	NI	NI
	50	NI	NI	NI	NI
5b	1000	10	NI	9	10
	500	9	NI	9	9
	250	7	NI	8	7
	125	7	NI	NI	7
	50	NI	NI	NI	NI
Amoxicillin	1000	17	15	40	35
	500	14	12	36	30
	250	14	12	31	28
	125	12	10	29	22
	50	9	9	25	20

NI: No Inhibition

**Table 2.** Evaluation of analgesic activity by the hot plate method

Group	Reaction Time (Seconds)	Inhibition (%)
<b>Standard</b>	13.41 ± 1.84 ***	73
<b>Control</b>	3.62 ± 0.74	
<b>1a</b>	4.35 ± 0.95	16
<b>1b</b>	6.08 ± 1.02 *	40
<b>4a</b>	5.33 ± 0.81	32
<b>4b</b>	6.63 ± 0.73 *	45
<b>5a</b>	7.36 ± 1.14 **	51
<b>5b</b>	4.09 ± 0.86	10

Each value is mean ±S.D. for six mice, \*p <0.05, \*\*p <0.01, \*\*\*p <0.001 compared with normal control. Data were analyzed by using one-way ANOVA followed by a T-test

**Table 3.** Evaluation of analgesic activity by the writhing method

Group	Number of Writhing	Inhibition (%)
<b>Standard</b>	12.36 ± 3.25 ***	71
<b>Control</b>	42.36 ± 4.47	
<b>1a</b>	13.95 ± 2.58 ***	68
<b>1b</b>	29.65 ± 5.24	30
<b>4a</b>	29.79 ± 4.21	30
<b>4b</b>	20.41 ± 3.62 **	52
<b>5a</b>	41.60 ± 7.08	3
<b>5b</b>	22.31 ± 3.69 *	47

Each value is mean ±S.D. for six mice, \*p <0.05, \*\*p <0.01, \*\*\*p <0.001 compared with normal control. Data were analyzed by using one-way ANOVA followed by a T-test

**Table 4:** Docking scores of synthesized compounds covalently bound to the active site of 6B73 protein and 5C1M protein

Compd.	Docking affinity (kcal/mol)			
	6B73	RMSD Å	5C1M	RMSD Å
<b>1a</b>	-6.89	1.05	-6.29	1.20
<b>1b</b>	-6.73	1.18	-6.56	1.98
<b>2b</b>	-4.90	1.17	-5.04	2.13
<b>2d</b>	-5.86	1.59	-5.54	1.10
<b>3</b>	-5.18	1.13	-4.94	1.39
<b>4a</b>	-8.48	1.77	-9.00	2.34
<b>4b</b>	-8.01	2.31	-9.21	1.34
<b>5a</b>	-8.00	2.11	-8.94	1.48
<b>5b</b>	-8.76	1.91	-8.86	2.13

**Table 5.** Molecular docking score, RMSD, and binding affinity for the compounds showed valid molecular docking scores with 6B73

Compd	S Score kcal/mol	RMSD Å	Bonds between Atoms of Compounds and Residues of Active Site of 6B73						
			Compd Atoms	Receptor Atoms	Receptor Residues	Interaction	d (Å)	E (kcal/mol)	Total E (kcal/mol)
1a	-6.89	1.05	Cl 33	O	HIS 291	H-donor	3.04	-0.1	-29.62
			O 25	CA	HIS 291	H-acceptor	3.29	-1.2	
1b	-6.73	1.18	O 25	CA	LYS 227	H-acceptor	3.45	-0.7	-27.51
			Cl 36	NZ	LYS 227	H-acceptor	3.95	-0.8	
			C 29	5-ring	HIS 291	H-pi	3.90	-2.4	
2b	-4.90	1.17	-	-	-	-	-	-	-23.28
2d	-5.86	1.59	S 16	OD1	ASP 138	H-donor	3.76	-1.2	-24.60
3	-5.18	1.13	S 1	SD	MET 142	H-donor	4.04	-1.0	-24.47
			5-ring	CZ3	TRP 287	pi-H	3.95	-0.8	
4a	-8.48	1.77	O 32	N	LEU 212	H-acceptor	3.22	-2.7	-46.83
			5-ring	NZ	LYS 227	pi-cation	3.64	-0.8	
			6-ring	6-ring	TYR 139	pi-pi	3.82	0	
4b	-8.01	2.31	S 38	O	CYS 210	H-donor	4.00	-0.4	-45.79
			O 3	NE2	GLN 115	H-acceptor	3.02	-2.3	
			N 34	NE2	GLN 115	H-acceptor	3.06	-1.4	
5a	-8.00	2.11	S 33	OD2	ASP 138	H-donor	4.10	-0.5	-36.34
			6-ring	NZ	LYS 227	pi-cation	4.25	-1.2	
5b	-8.76	1.91	O 32	N	LEU 212	H-acceptor	2.98	-1.7	-46.85

**Table 6.** Molecular docking score, RMSD, and binding affinity for the compounds showed valid molecular docking scores with 5C1M

Compd	S Score kcal/mol	RMSD Å	Bonds between Atoms of Compounds and Residues of Active Site of 5C1M						
			Compd Atoms	Receptor Atoms	Receptor Residues	Interaction	d (Å)	E (kcal/mol)	Total E (kcal/mol)
1a	-6.29	1.20	N 22	SD	MET 151	H-donor	4.40	-1.4	-30.44
			C 26	SD	MET 151	H-donor	3.80	-0.8	
1b	-6.56	1.98	C 33	5-ring	HIS 297	H-pi	3.60	-0.7	-29.17
			5-ring	5-ring	HIS 54	pi-pi	3.92	0	
2b	-5.04	2.13	S 16	O	HIS 54	H-donor	3.63	-3.2	-22.10
			5-ring	5-ring	HIS 54	pi-pi	3.66	0	
2d	-5.54	1.10	N 12	SD	MET 151	H-donor	3.71	-0.5	-22.43
			C 1	5-ring	HIS 297	H-pi	4.12	-1.0	
			5-ring	6-ring	TYR 148	pi-pi	3.48	0	
3	-4.94	1.39	S 1	O	ASP 147	H-donor	3.68	-0.7	-21.48
4a	-9.00	2.34	O 3	CE	LYS 233	H-acceptor	3.13	-0.9	-45.89
			6-ring	CG2	VAL 300	pi-H	4.40	-0.7	
			5-ring	CD	LYS 303	pi-H	4.00	-0.9	
4b	-9.21	1.34	C 29	SD	MET 151	H-donor	3.89	-0.8	-48.66
			6-ring	CE	LYS 303	pi-H	4.64	-0.6	
			5-ring	5-ring	HIS 54	pi-pi	3.66	0	
5a	-8.94	1.48	N 26	O	HIS 54	H-donor	3.11	-2.3	-46.21
			6-ring	CB	SER 53	pi-H	3.95	-1.0	
			5-ring	CA	HIS 54	pi-H	3.95	-1.2	
			5-ring	5-ring	HIS 54	pi-pi	3.97	0	
5b	-8.86	2.13	O 3	CB	LYS 233	H-acceptor	3.27	-1.1	-46.52
			5-ring	CE	SER 53	pi-H	4.01	-0.6	